

BEAM DYNAMICS OPTIMIZATION OF LCLS-II-HE LINEAR ACCELERATOR DESIGN*

J. Qiang[†], LBNL, Berkeley, CA, USA

T. Raubenheimer, M. Woodley, SLAC, Menlo Park, CA, USA

Abstract

The LCLS-II-HE as a high energy upgrade of the high repetition rate X-ray FEL under construction at SLAC will provide great opportunities for scientific discovery by generating coherent, high brightness hard X-ray radiation. In this paper, we report on beam dynamics optimization of the LCLS-II HE linear accelerator design with a 100 pC and a 20 pC charge beam to attain high quality electron beam for X-ray FEL radiation. We also present preliminary results of beam dynamics optimization of a 100 pC beam from a low emittance superconducting injector.

INTRODUCTION

The high brightness, coherent X-ray Free Electron Laser (FEL) provides an important tool for scientific discoveries in basic energy science. The LCLS-II-HE as a high energy upgrade of the high repetition rate X-ray FEL, LCLS-II [1, 2], will increase the final electron beam energy from 4 GeV to 8 GeV and photon spectral range to 12.8 keV with potential to be extended through 20 keV with improvements of the electron injector and beam transport [3]. In order to attain shorter wavelength X-ray radiation, the electron beam quality at the entrance of radiation undulator needs to be optimized. In this paper, we report on the beam dynamics optimization of electron beam transport through a recent LCLS-II-HE linear accelerator design lattice using a 100 pC and a 20 pC charge electron beam from the LCLS-II injector, and a 100 pC charge beam from a low emittance superconducting injector.

COMPUTATIONAL MODEL

The LCLS-II-HE beam dynamics optimization using the IMPACT code starts with an initial distribution at the exit of the LCLS-II injector. This is based on the assumption that there is no upgrade of the injector design in the HE project. The IMPACT code is a massive parallel particle-in-cell code for modeling high intensity/high brightness beams in linear and circular accelerators [4-6]. The computational model in the IMPACT code includes exact transfer map through a drift, linear transfer map for hard edge quadrupole with energy dependence, 5th order transfer map through dipole, linear transfer matrix through RF superconducting cavity, thin lens kick model for sextupole, self-consistent 3D space-charge effects, 1D steady state and transient coherent synchrotron radiation (CSR) effects, incoherent synchrotron radiation (ISR) effects through a bending magnet, longitudinal structure and resistive wall

wakefields, and uncorrelated energy increase from an analytical intrabeam scattering (IBS) model. The IMPACT code has been successfully applied to light source modeling and benchmarked with both the other code and experimental measurements [7-9]. In this study, we have used real number of electrons in the simulation to capture the initial shot-noise of the beam and 64x64x2048 computational grid points to calculate the 3D space-charge effects. The accelerator lattice is based on the MAD input file of July, 2020.

BEAM DYNAMICS OPTIMIZATION WITH 100 pC CHARGE

The beam dynamics optimization of the LCLS-II-HE linear accelerator in this section used an initial particle distribution from the LCLS-II injector. The linear accelerator consists of a laser heater (LH) to suppress microbunching instability, a section of superconducting linac L1, a bunch compressor BC1, a second section of superconducting linac L2, a bunch compressor BC2, a third section of superconducting linac L3, and a fourth section of superconducting linac to accelerate the beam to 8 GeV, a long bypass transport line, and a magnetic kicker to spread the electron beam to a soft X-ray transport beam line and to a hard X-ray transport beam line. The superconducting linacs in all four sections are made of 1.3 GHz 9 cell superconducting cavities except the two cryomodules of 3.9 GHz third harmonic cavities right before the BC1 to linearize longitudinal phase space.

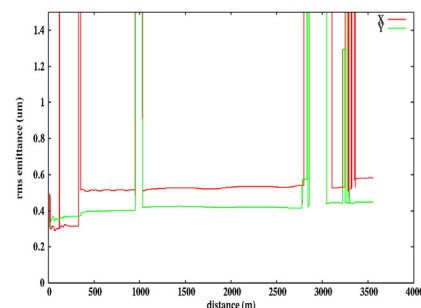


Figure 1: Transverse projected emittance evolution through the accelerator and the hard X-ray beam line (100 pC).

We tuned quadrupole settings in front of the laser heater, after the laser heater, and quadrupole settings after the BC1 to match the distribution to the designed Twiss parameters including the space-charge effects of the 100 pC beam. Figure 1 shows electron beam transverse RMS projected emittance evolution through the linear accelerator and the hard X-ray beam line. The transverse emittances are reasonably well preserved with less than 0.6 μm final horizontal and over 0.4 μm vertical emittances. The major

*Work supported by the Director of the Office of Science of the US Department of Energy under Contract no. DEAC02-05CH11231.

[†]jqiang@lbl.gov

horizontal emittance growth occurs after BC2 due to the coherent synchrotron radiation (CSR) effects from large longitudinal bunch compression. Figure 2 shows the final longitudinal phase space distribution and current profile at entrance to the hard X-ray undulator radiation section. It is seen that the electron beam has a section of about 10 μm flat core inside the distribution. The peak current inside this core after removing the fold-in particles is about 1.4 kA. This longitudinal distribution was attained through optimizing the RF cavity phase and amplitude in L1, L2, and L3, and bending angles in BC1 and BC2 [10, 11].

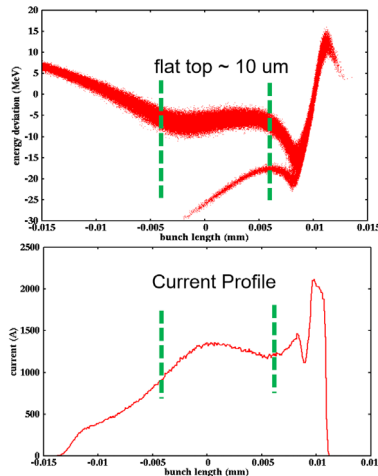


Figure 2: Final longitudinal phase space distribution and current profile at the entrance of the hard X-ray undulator.

Figure 3 shows the final transverse slice emittances at entrance of the hard X-ray undulator. The final slice emittances inside the core of the electron beam distribution are around 0.25 μm . As a summary, we list the final electron beam parameters at the undulator entrance in Table 1 for the 100 pC charge through both hard X-ray and soft X-ray beam lines.

In both cases, high brightness electron beams with more than 1.2 kA averaged (inside the core) current, ~ 1 MeV uncorrelated energy spread, and $\sim 0.25 \mu\text{m}$ emittances were attained after the beam dynamics optimization.

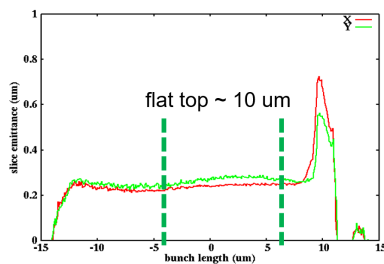


Figure 3: Final slice emittance at the entrance of the hard X-ray undulator (100 pC).

Table 1: Final Electron Beam Parameters (100 pC)

IMPACT Studies	I_{core} (A)	σ_E (keV)	Proj. e_x/e_y (mm-mrad)	Slice e_x/e_y (mm-mrad)
HXR	1238	1025	0.58 / 0.45	0.24 / 0.27
SXR	1251	1034	0.53 / 0.43	0.25 / 0.27

BEAM DYNAMICS OPTIMIZATION WITH 20 pC CHARGE

We applied the same beam dynamics optimization procedure of the linear accelerator with 20 pC charge from the LCLS-II injector. Figure 4 shows transverse projected RMS emittance evolution through the accelerator and the hard X-ray beam line. The transverse emittances are well preserved through the accelerator beam deliverable system with less than 0.2 μm final emittances. The major horizontal emittance growth occurs after the BC1 due to the CSR effects from large compression.

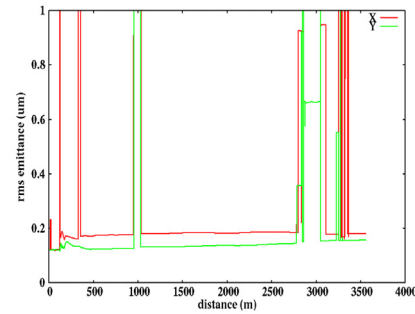


Figure 4: Transverse projected emittance evolution through the accelerator and the hard X-ray beam line (20 pC).

Figure 5 shows the final longitudinal phase space distribution and current profile at the entrance of the hard X-ray undulator. A relatively flat longitudinal core with about 6 μm long was attained from the beam dynamics optimization. The peak current inside the core of the electron beam distribution is over 500 A.

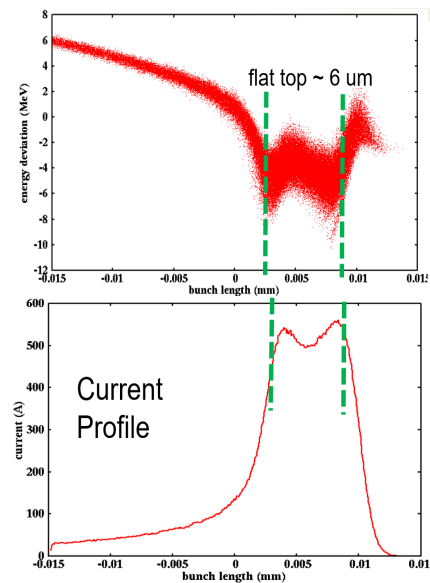


Figure 5: Final longitudinal phase space distribution and current profile at the entrance of the hard X-ray undulator.

Figure 6 shows the final transverse slice emittances at the entrance of the hard X-ray beam line. The slice emittances vary inside the core with a maximum less than 0.2 μm . The final electron beam parameters at the entrance of both hard X-ray and soft X-ray beam lines for the 20 pC charge are summarized in Table 2. A high brightness electron beam

with final ~ 520 A averaged (inside the core) current, 1 MeV uncorrelated energy spread, and less than $0.2 \mu\text{m}$ transverse emittances was attained in both cases.

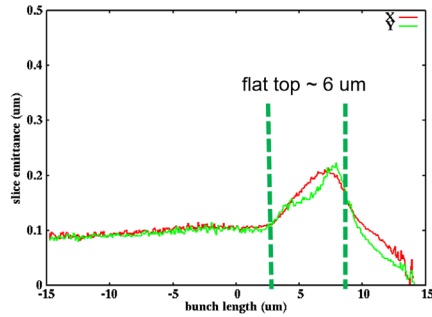


Figure 6: Final transverse slice emittance at the entrance of the hard X-ray undulator (20 pC).

Table 2: Final Electron Beam Parameters (20 pC)

IMPACT Studies	I_{core} (A)	σ_E (keV)	Proj. e_x/e_y (mm-mrad)	Slice e_x/e_y (mm-mrad)
HXR	521	1018	0.18 / 0.16	0.17 / 0.17
SXR	521	1025	0.19 / 0.15	0.18 / 0.17

BEAM DYNAMICS OPTIMIZATION WITH 100 pC CHARGE FROM LOW EMITTANCE INJECTOR

In order to attain shorter X-ray wavelength radiation of 20 keV, the electron beam brightness needs to be further improved. A new low emittance injector based on superconducting RF gun is being actively studied at SLAC. Such an injector can generate a 100 pC electron beam with transverse emittance as low as about $0.1 \mu\text{m}$. In this study, we used a particle distribution from the low emittance injector and carried out the same beam dynamics optimization of the linear accelerator.

Figure 7 shows the transverse projected emittance evolution through the accelerator and the hard X-ray beam line. The initial small emittances were reasonably well preserved through the accelerator beam delivery system with around $0.25 \mu\text{m}$ final horizontal emittance and $0.15 \mu\text{m}$ final vertical emittance. The major horizontal emittance growth occurs after BC2 due to the CSR effects from the large longitudinal compression. The major vertical emittance growth occurs after BC1 due to mismatched space-charge effects.

Figure 8 shows the final longitudinal phase space distribution and current profile at the entrance of the hard X-ray undulator section. A $10 \mu\text{m}$ reasonably flat core of electron beam was obtained after the optimization. The peak current inside this core reaches 1.6 kA. Small fluctuation of particle distribution inside the core is due to numerical microbunching instability effects with the use of small number of macroparticles (100,000) in this simulation. This can be mitigated with the use of real number of electrons in the start-to-end simulation and the

heating of the uncorrelated energy spread from the laser heater.

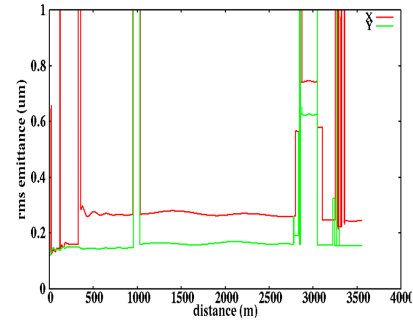


Figure 7: Transverse projected emittance evolution through the accelerator and the hard X-ray beam line (100 pC).

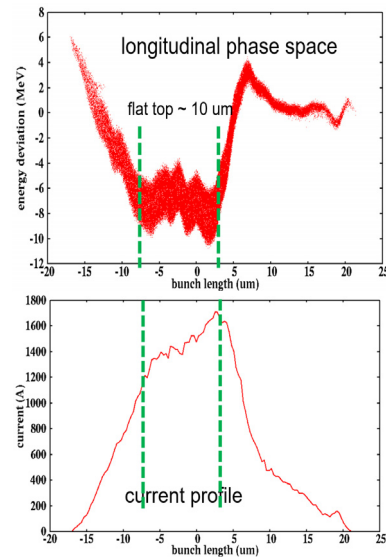


Figure 8: Final longitudinal phase space distribution and current profile at the entrance of hard X-ray undulator.

Figure 9 shows the final transverse slice emittances at the entrance of the hard X-ray undulator. Both horizontal and vertical slice emittances inside the core of the beam are below $0.15 \mu\text{m}$. Such a high brightness electron beam will help to extend the X-ray radiation energy up to 20 keV.

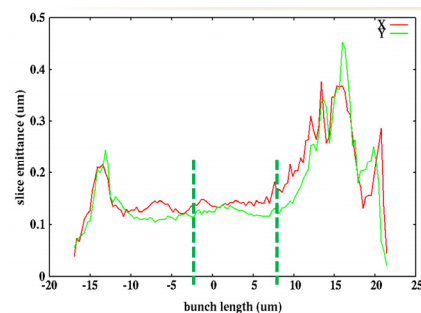


Figure 9: Final slice emittance at the entrance of the hard X-ray undulator (100 pC).

ACKNOWLEDGEMENTS

We would like to thank Dr. Fuhao Ji and the injector team for the initial particle distribution from the superconducting low emittance injector.

REFERENCES

- [1] T. O. Raubenheimer, “LCLS-II: Status of the CW X-ray FEL Upgrade to the LCLS Facility”, in *Proc. 37th Int. Free Electron Laser Conf. (FEL'15)*, Daejeon, Korea, Aug. 2015, pp. 618-624. doi:10.18429/JACoW-FEL2015-WEP014
- [2] “LCLS-II Conceptual Design Report”, SLAC National Accelerator Lab., Menlo Park, CA, USA, Rep. SLAC-R-1092, Jan. 2014.
- [3] T. O. Raubenheimer, “The LCLS-II-HE, A High Energy Upgrade of the LCLS-II”, in *Proc. 60th ICFE Advanced Beam Dynamics Workshop on Future Light Sources (FLS'18)*, Shanghai, China, Mar. 2018, pp. 6-11. doi:10.18429/JACoW-FLS2018-MOP1WA02
- [4] J. Qiang, R. Ryne, S. Habib, and V. Decyk, “An Object-Oriented Parallel Particle-In-Cell Code for Beam Dynamics Simulation in Linear Accelerators”, *J. Comp. Phys.*, vol. 163, pp. 434-451, 2000. doi:10.1006/jcph.2000.6570
- [5] J. Qiang, S. Lidia, R. D. Ryne, and C. Limborg-Deprey, “A Three-Dimensional Quasi-Static Model for High Brightness Beam Dynamics simulation”, *Phys. Rev. ST Accel. Beams*, vol. 9, p. 044204, 2006. doi:10.1103/physrevstab.9.044204
- [6] J. Qiang, R. D. Ryne, M. Venturini, A. A. Zholents, and I. V. Pogorelov “High resolution simulation of beam dynamics in electron linacs for x-ray free electron lasers”, *Phys. Rev. ST Accel. Beams*, vol. 12, p. 100702, 2009. doi:10.1103/physrevstab.12.100702
- [7] J. Qiang *et al.*, “Start-to-end simulation of X-ray radiation of a next generation light source using the real number of electrons”, *Phys. Rev. ST Accel. Beams*, vol. 17, p. 030701, 2014. doi:10.1103/physrevstab.17.030701
- [8] J. Qiang *et al.*, “Start-to-end simulation of the shot-noise driven microbunching instability experiment at the Linac Coherent Light Source”, *Phys. Rev. Accel. Beams*, vol. 20, p. 054402, 2017. doi:10.1103/physrevaccelbeams.20.054402
- [9] L. Wang, P. Emma, T. O. Raubenheimer, and J. Qiang, “Benchmark of ELEGANT and IMPACT”, in *Proc. 37th Int. Free Electron Laser Conf. (FEL'15)*, Daejeon, Korea, Aug. 2015, pp. 505-507. doi:10.18429/JACoW-FEL2015-TUP066
- [10] J. Qiang, “Advances in Global Optimization of High Brightness Beams”, *International Journal of Modern Physics A*, vol. 34, p. 1942016, 2019. doi:10.1142/s0217751x19420168
- [11] J. Qiang, “Fast longitudinal beam dynamics optimization in x-ray free electron laser linear accelerators”, *Phys. Rev. Accel. Beams*, vol. 22, p. 094401, 2019. doi:10.1103/physrevaccelbeams.22.094401